European Heart Journal – Cardiovascular Imaging (2014) **15**, 500–508
doi:10.1093/ehjci/jet191

Mechanisms of atrial mitral regurgitation: insights using 3D transoesophageal echo

Liam Ring[1]*, David P. Dutka[1], Francis C. Wells[2], Simon P. Fynn[2], Leonard M. Shapiro[2], and Bushra S. Rana[2]

[1]Department of Medicine, University of Cambridge, Addenbrookes Hospital, Hills Road, Cambridge CB2 0QQ, UK; and [2]Papworth Hospital NHS Foundation Trust, Papworth Everard, Cambridge CB23 3RE, UK

Received 29 May 2013; revised 19 August 2013; accepted after revision 26 September 2013; online publish-ahead-of-print 20 October 2013

Aims Functional mitral regurgitation (FMR) is a consequence of mitral annular enlargement, leaflet tethering and reduced co-aptation. The importance of the left atrium (LA) as a cause of mitral regurgitation (MR) is less clear. We applied a co-aptation index using three-dimensional (3D) transoesophageal echocardiography to FMR and MR secondary to LA dilatation (atrial mitral regurgitation, AMR).

Methods and results Seventy-two patients underwent comprehensive 3D echo studies: FMR ($n = 19$); AMR ($n = 33$); and 20 controls. We recorded: LV size and function; LA dimensions; mitral annular area (MVA); and leaflet area in early and late systole. MVA fractional change was defined: (MVA late systole − MVA early systole)/MVA late systole × 100%; the co-aptation index was defined: (leaflet area early systole − leaflet area late systole)/leaflet area early systole × 100%. Despite normal LV size and function in AMR, MVA was increased similarly to FMR (AMR 12.86 cm^2 vs. FMR 12.33 cm^2, $P = ns$; both $P < 0.01$ vs. controls 8.83 cm^2), and MVA fractional change similarly reduced (AMR 5.1% vs. FMR 6.3%; $P = ns$; both $P < 0.001$ vs. controls 14.6%). The co-aptation index was reduced in both MR groups (FMR 6.6% vs. AMR 7.0%, $P = ns$; both $P < 0.001$ vs. controls 19.6%). After multivariate analysis, the co-aptation index ($\chi^2 = 41.2$) and MVA fractional change ($\chi^2 = 22.1$) remained the strongest predictors of MR (both $P < 0.001$ for the model). A co-aptation index of $\leq$13% was 96% sensitive and 90% specific for the presence of MR.

Conclusion LA dilatation leads to MVA enlargement, reduced leaflet co-aptation and MR even without LV dilatation. A co-aptation index describes this *in vivo*. This work provides insights into the mechanism of AMR.

Keywords mitral valve regurgitation • three-dimensional transoesophageal echocardiography • left atrium

Introduction

Functional mitral regurgitation (FMR) occurs in non-ischaemic or ischaemic left ventricular (LV) dysfunction.[1–3] Mitral annular enlargement contributes to the presence of mitral regurgitation (MR) in these patients, but previous work suggests that the dominant mechanism of MR is displacement of the subvalve apparatus resulting in failure of optimal co-aptation of the mitral valve leaflets.[4–8] Two-dimensional echocardiography measures the displacement of the leaflets into the ventricle in a single plane, but it does not describe the interaction of the leaflets across the width of the valve. The advent of three-dimensional (3D) echocardiography enables the mitral valve to be visualized in its entirety: previous work used a novel co-aptation index to describe the interaction between the anterior and posterior mitral valve leaflets at the co-aptation zone.[9] This technique was able to predict the development of valvular insufficiency through loss of optimal leaflet co-aptation in animal models of FMR.

Conversely, the left atrium (LA) has been neglected as a potential cause of MR. LA dilatation is frequently seen in patients with MR, but is generally considered the consequence, opposed to the cause, of valvular insufficiency. Previous studies have concluded that LA enlargement may result in mitral annular dilatation, but there are conflicting views as to whether this alone will result in MR.[10–13] More recent work has highlighted the importance of atrial fibrillation (AF) as a cause of 'atrial mitral regurgitation' (AMR).[14] We hypothesized that patients with isolated atrial dilatation would display annular dilatation and impaired co-aptation determined using 3D

* Corresponding author. Tel: +44 1223 331504; Fax: +44 1223 331505, Email: liamring@doctors.org.uk
Published on behalf of the European Society of Cardiology. All rights reserved. © The Author 2013. For permissions please email: journals.permissions@oup.com

Downloaded from https://academic.oup.com/ehjcimaging/article/15/5/500/2399644 by U.S. Department of Justice user on 17 August 2022

transoesophageal echocardiography (TOE). Additionally, we sought to determine whether annular function contributes to loss of co-aptation and the presence of MR in these patients.

Methods

Patient population

We identified patients with at least moderate MR undergoing TOE between February 2010 and October 2012. We excluded patients with prior mitral valve surgery. Patients in whom MR was secondary to global or regional LV dysfunction were labelled as FMR according to a previous definition[7] (*Figure 1*). Patients were labelled as AMR if they fulfilled the following criteria: (i) normal LV size and function without regional wall motion abnormalities; (ii) morphologically normal mitral valve leaflets without evidence of prolapse or stenosis, and (iii) dilated left atria, defined according to European guidelines as left atrial volumes of >52 mL (females) and >58 mL (males; *Figure 2*).[15] Comparison was made with 20 patients, all of whom were investigated to rule out a cardiac source of embolism and were found to have a normal heart, including normal LV size and function, normal LA volume, and a structurally normal mitral valve with less than mild MR. The study was granted institutional approval by the Papworth Hospital NHS Foundation Trust (*Figure 3*).

Image acquisition

Images were acquired using an iE33 imaging platform with S5-1 and X7-2t transducers (Philips, Andover, MA, USA), and analysed offline using Xcelera (Philips). From the parasternal long-axis window, we recorded LV end-diastolic and end-systolic diameters (LVIDd and LVIDs). LA volume, LV end-systolic volume, and LV ejection fraction (EF) were determined using Simpson's Biplane method from apical windows. Diastolic function was described with the *E*/*E′* ratio, where *E* was measured using pulsed Doppler of the mitral inflow from the four-chamber view, and *E′* as the average of the septal and lateral mitral annular diastolic velocities using tissue Doppler imaging. The presence of moderate MR was defined using a multiparametric approach including assessment of the effective regurgitant orifice area (EROA) using the Proximal Isovelocity Surface Area (PISA) method, the vena contracta, and pulmonary venous flow reversal.[16] An EROA was used for comparison between groups. In all patients, the TOE study was performed under conscious sedation, ensuring that systolic blood pressure was maintained throughout the examination. The 3D datasets were acquired from the mid-oesophagus using the live 3D or 3D zoom functions and analysed according to current guidelines.[17] Sector width, gain, and depth settings were adjusted to ensure that the entire mitral valve annulus was included (frame rate of >8 fps). We acquired two consecutive beats, and datasets analysed offline using the dedicated software (QLab, Mitral Valve Quantification, Philips). First, the end-systolic frame was selected, defined as the last frame prior to mitral valve opening. We manually identified the inter-commissural (IC) and antero-posterior (AP) diameter, and subsequently defined the hingepoints of the leaflets in eight rotational planes before the leaflets were traced in parallel slices across the valve. Mitral annular parameters recorded included: AP and IC diameter, annular height, and area (MVA). From these, we derived the annular height to IC ratio (AHICR, defined as annular height/IC diameter), a measure of the non-planarity of the mitral annulus independent of annular size, or patients' body surface area. In addition, measures of leaflet geometry were recorded including tenting height, tenting volume, and total leaflet surface area. Finally, we identified early systole, defined as the first frame in which the mitral leaflets were seen to co-apt (*Figure 4*). The above procedure was repeated, and we recorded the MVA and total leaflet surface area in early systole. We defined the fractional area change of MVA as: (MVA late systole − MVA early systole)/MVA late systole × 100%. The co-aptation index is a three-dimensional assessment of the surface area of co-aptation, i.e. the total area of 'overlap' between the anterior and posterior mitral valve leaflets during systole. This value is indexed to the size of the valve, thus providing an assessment of co-aptation that is independent of the patient's body surface area. This was calculated as previously described[9] as: (leaflet surface area early systole − leaflet surface area late systole)/leaflet surface area early systole × 100%.

Statistical analysis

Data were analysed using SPSS v19.0 (SPSS, Inc., Chicago, IL, USA). Values are expressed as mean ± SD. Continuous parameters were checked for the normality of distribution using the Shapiro–Wilk test, and compared using the one-way analysis of variance (ANOVA) with post-test Bonferroni correction. Non-normally distributed data were compared using the Kruskal–Wallis test with post-hoc Dunn correction for multiple comparisons. Associations between annular size and function were determined with linear regression analysis. Clinical and echocardiographic characteristics, including age, gender, rhythm, LV dimensions in diastole and systole,

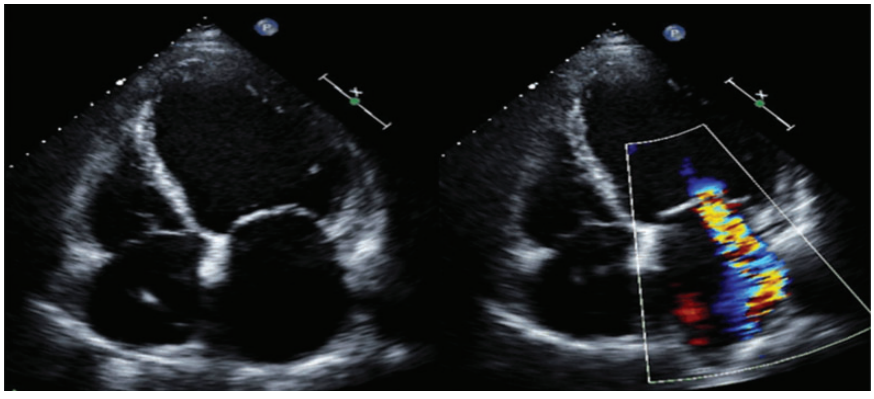

Figure 1 Typical 2D transthoracic echo image of a patient with functional MR (left). Note the dilated left ventricle, and the displacement of the mitral leaflets into the left ventricle. This results in significant MR (right).

Downloaded from https://academic.oup.com/ehjcimaging/article/15/5/500/2399644 by U.S. Department of Justice user on 17 August 2022

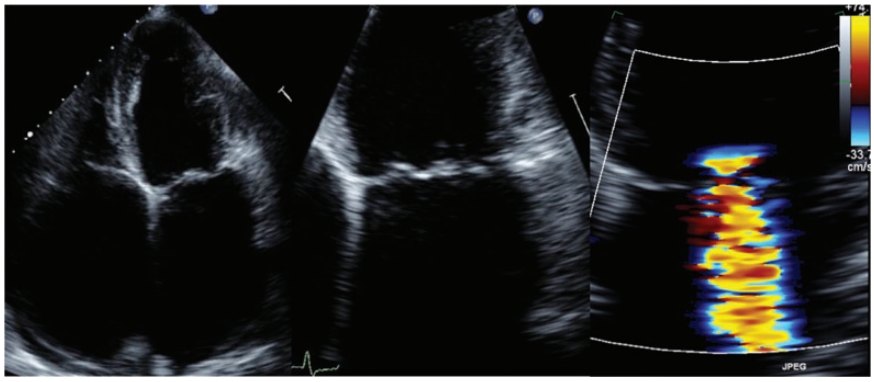

Figure 2 Left pane depicts a 2D transthoracic image of a patient with atrial MR. Both atria are significantly dilated, but the LV dimensions are normal. In the zoomed image (centre), note how the mitral leaflets sit almost level with the annular plane: there is no tenting or prolapse. The image on the right shows the associated regurgitation.

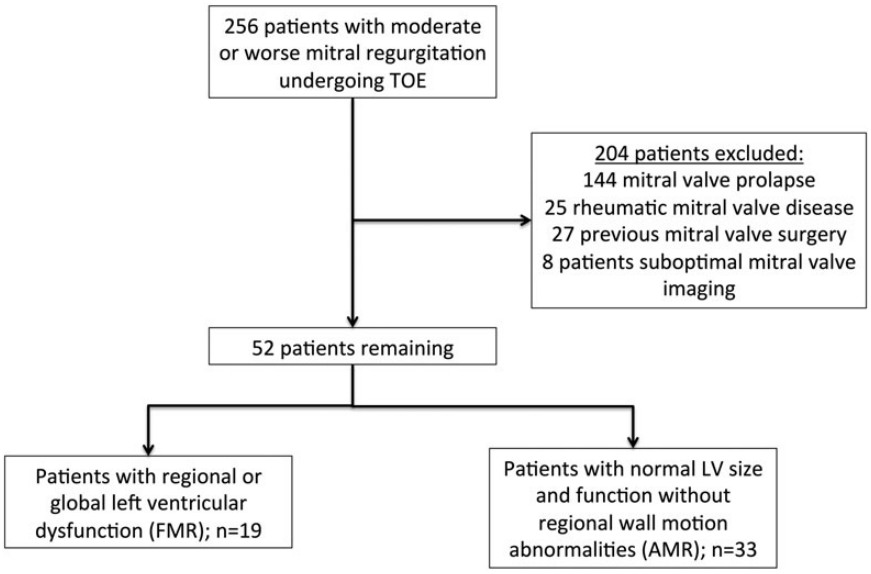

Figure 3 Flow diagram of patients included in analysis. FMR: functional mitral regurgitation; AMR: atrial mitral regurgitation.

EF, and left atrial volume, were entered into separate univariate and multivariate models with the annular size and annular contraction as the dependent variable. Independent associations are described as the β co-efficient and the 95% confidence intervals, with the model r^2 for the explained variance.

To determine clinical and echocardiographic factors predictive of MR, we employed multivariate regression analysis. Factors found to be significant or borderline on univariate analysis ($P \leq 0.10$) were subsequently entered into a multivariate forward stepwise model. Receiver-operator characteristic curves were constructed to evaluate the contributions of variables to the presence of MR. Optimal values were defined as those with best sensitivity and specificity. Intra- and inter-observer variability was described by the co-efficient of variation, and 95% limits of agreement of the absolute values were calculated using a Bland–Altman analysis. *P*-values of <0.05 were considered statistically significant.

Results

Complete datasets were available for 52 patients: 19 were labelled as FMR (10 males; age 72 $\pm$ 7 years), and 33 as AMR (16 males; age 71 $\pm$ 7 years). Most were in AF (AMR 82% and FMR 63%). Baseline characteristics are listed in *Table 1*. For those AMR patients not in AF, the aetiology of left atrial enlargement was hypertension. In the FMR cohort, the underlying aetiology was ischaemic heart disease in 8 (42%), and non-ischaemic cardiomyopathy in the remaining 11 (58%). In addition to the presence of MR, 25 (76%) patients in the AMR group had at least moderate tricuspid regurgitation (TR), and 3 (9%) had moderate aortic stenosis. For the FMR cohort, 12 (63%) patients had at least moderate TR, and 1 had moderate aortic stenosis.

Downloaded from https://academic.oup.com/ehjcimaging/article/15/5/500/2399644 by U.S. Department of Justice user on 17 August 2022

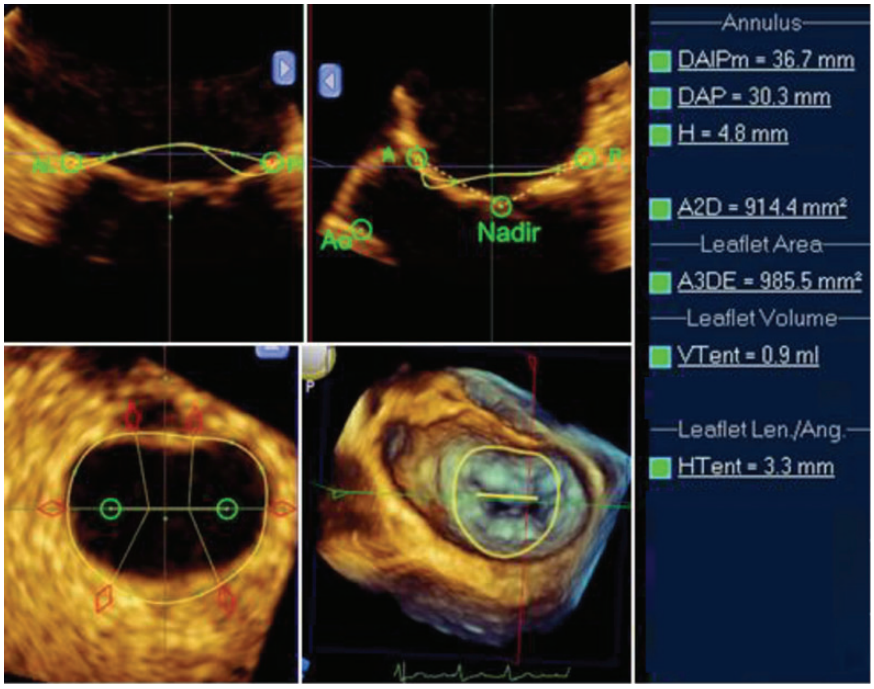

Figure 4 Typical Mitral Valve Quantification (MVQ) analysis image of a patient with AMR. The mitral annulus is displayed in three orthogonal planes, with the 3D image to aid orientation (bottom right pane). On the right, the software displays the values for annular parameters, including IC diameter (DAIP); antero-posterior diameter (DAP); annulus height (H); annular area (A2D); total leaflet surface area (A3DE); tenting volume (VTent), and tenting height (HTent). To determine the co-aptation index, the analysis is performed in early systole (displayed here) and repeated in end-systole.

Table 1 Baseline characteristics

	Controls ($n = 20$)	*P*-value (controls vs. AMR)	AMR ($n = 33$)	*P*-value (AMR vs. FMR)	FMR ($n = 19$)
Male/female	12/8	Ns	16/17	Ns	10/9
Age (years)	52 ± 16	<0.001	71 ± 7	Ns	72 ± 7*
Body surface area (m^2)	1.9 ± 0.2	Ns	1.9 ± 0.2	Ns	1.9 ± 0.3
Rhythm (sinus rhythm/AF)	20/0	<0.001	6/27	Ns	7/12*
LVIDd (mm)	48 ± 5	Ns	51 ± 6	0.001	58 ± 6*
LVIDs (mm)	31 ± 3	Ns	33 ± 6	<0.001	44 ± 6*
LVESV (mL)*	35 ± 11	Ns	39 ± 13	<0.001	74 ± 16*
Left atrial volume (mL)*	40 ± 9	<0.001	127 ± 61	Ns	112 ± 51*
EF (%)	63 ± 4	Ns	62 ± 5	<0.001	38 ± 6*
E/E′	9.0 ± 2.3	Ns	10.8 ± 3.9	0.02	16.1 ± 7.7*
Additional valvular pathology					
TR, *n* (%)			25 (76)	Ns	12 (63)
AVD, *n* (%)			3 (9)	Ns	1 (6)
MR severity					
EROA (cm^2)*			0.23 ± 0.13	0.111	0.32 ± 0.18

Data are compared using the ANOVA or Kruskal–Wallis where appropriate.
AMR: atrial mitral regurgitation; FMR: functional mitral regurgitation; AF: atrial fibrillation; LVIDd: left ventricular internal diameter diastole; LVIDs: left ventricular internal diameter systole; LVESV: left ventricular end-systolic volume; EF: ejection fraction; LAD: left atrial diameter; TR: tricuspid regurgitation; AVD: aortic valve disease; MR: mitral regurgitation; EROA: effective regurgitant orifice area.
*$P < 0.001$ FMR vs. controls.

Downloaded from https://academic.oup.com/ehjcimaging/article/15/5/500/2399644 by U.S. Department of Justice user on 17 August 2022

Table 2 Mitral annular parameters

	Controls ($n = 20$)	*P*-value (control vs. AMR)	AMR ($n = 25$)	*P*-value (AMR vs. FMR)	FMR ($n = 19$)
Annular parameters (end-systole)					
MVA (cm^2)	8.83 ± 1.27	<0.001	12.86 ± 3.47	Ns	12.33 ± 1.98*
AP diameter	29 ± 3	<0.001	36 ± 5	Ns	36 ± 4*
IC diameter	35 ± 3	<0.001	42 ± 5	Ns	42 ± 3*
Annular height (mm)	5.6 ± 1.8	Ns	5.6 ± 1.6	Ns	5.9 ± 1.5
AHICR (%)	15.9 ± 4.4	Ns	13.6 ± 4.5	Ns	14.1 ± 3.1
Leaflet parameters (end-systole)					
Tenting height (mm)	4.7 ± 1.1	<0.05	3.5 ± 1.5	<0.001	8.1 ± 2.4*
Tenting volume (mls)	1.2 ± 0.4	Ns	1.0 ± 0.7	<0.001	3.4 ± 1.6*
Total leaflet surface area (cm^2)	9.34 ± 1.47	<0.001	14.09 ± 3.90	Ns	14.45 ± 2.53*
MVA fractional change (%)	14.6 ± 5.0	<0.001	5.1 ± 4.5	Ns	6.3 ± 5.3*
Co-aptation index (%)	19.6 ± 7.4	<0.001	7.0 ± 3.4	Ns	6.6 ± 3.8*

Data are compared using the ANOVA or Kruskal–Wallis where appropriate.
MVA: mitral annular area; AP: antero-posterior; IC: inter-commissural; AHICR: annular height to inter-commissural ratio; other abbreviations as previously.
*$P < 0.001$ FMR vs. controls.

As expected by design, FMR patients had increased LV dimensions and lower EF compared with AMR and control patients. Similarly, the *E/E′* ratio was significantly elevated in FMR, whereas it was comparable with AMR and controls (*Table 1*). LA volumes were similarly enlarged in FMR and AMR (FMR LA volume 112 ± 51 mL vs. AMR 127 ± 61 mL, $P =$ ns; both $P < 0.001$ vs. controls 40 ± 9 mL; *Table 1*). There was no difference in the severity of MR between those patients with FMR and AMR (EROA 0.32 ± 0.18 vs. 0.23 ± 0.13 cm^2; $P = 0.11$).

Annular parameters

The mean frame rate of 3D datasets was 12 (range 8–25) fps. Despite normal LV systolic volumes in AMR, MVA was similarly enlarged in AMR and FMR (AMR 12.86 ± 3.47 cm^2 vs. FMR 12.33 ± 1.98 cm^2, $P =$ ns; both $P < 0.001$ vs. controls 8.83 ± 1.27 cm^2). This pattern is replicated in the AP and IC values (*Table 2*). Fractional MVA change was similarly reduced in AMR and FMR, compared with controls (AMR 5.1 ± 4.5% vs. FMR 6.3 ± 5.3%, $P =$ ns; both $P < 0.001$ vs. controls 14.6 ± 5.0%; *Figure 5*).

AMR and FMR groups differed with regard to mitral annular geometry. Tenting height represents the lowest point of the mitral leaflets below the annular line at end-systole. This was increased in FMR, and lower in AMR than in normal controls (FMR 8.1 ± 2.4 mm vs. controls 4.7 ± 1.1 mm, $P < 0.001$; AMR 3.5 ± 1.5 mm, $P < 0.05$ vs. controls; *Table 2*). Finally, we determined the co-aptation index, which was similarly reduced in AMR and FMR compared with controls (*Figure 6*; AMR 7.0 ± 3.4% vs. FMR 6.6 ± 3.8%, $P =$ ns; both $P <$ 0.001 vs. controls 19.6 ± 7.4%).

Linear regression analysis was employed to explore the independent association between MV annular size and function. The strongest univariate associations of the MVA were left atrial volume ($r = 0.841$; $P < 0.001$), rhythm ($r = -0.51$, $P < 0.001$), and LV dimensions in diastole ($r = 0.479$; $P < 0.001$). After multivariate analysis, LA volume ($\beta = 0.03$; $P < 0.001$) in addition to rhythm and gender remained independently associated with MVA (*Table 3*). For annular fractional change, the strongest univariate associations were rhythm ($r = 0.606$; $P < 0.001$) and LA volume ($r = -0.556$; $P < 0.001$), both of which remained independent associations after multivariate analysis (*Table 3*). LV size was not an independent associate with either mitral annular area or annular fractional change.

To determine the predictors of MR, logistic regression analysis was employed. Univariate predictors of the presence of moderate MR were: age, LV dimensions, EF, left atrial dimensions, MVA, AP and IC diameter, AHICR, tenting volume, MVA fractional change, and the co-aptation index. These factors were subsequently incorporated into a forward stepwise multivariate model. After analysis, MVA fractional change and the co-aptation index remained the predictors of MR (co-aptation index: $\chi^2 = 41.2$; MVA fractional change: $\chi^2 = 22.1$; both $P < 0.001$ for the model). Using a receiver-operator characteristic curve, optimal cut-offs for these indices were determined. A co-aptation index of ≤13% displayed 96% sensitivity and 90% specificity for the presence of at least moderate MR, whereas an MVA fractional change of ≤11% displayed 87% sensitivity and 85% specificity for the same.

Measurement variability (95% limits of agreement and co-efficient of variation) for intra-observer differences were as follows: mitral annular area 3.1% ± 0.8 cm^2; tenting height 3.8% ± 0.6 mm; tenting volume 4.7% ± 0.2 mL; leaflet surface area 3.3% ± 0.9 cm^2; and co-aptation index 5.4 ± 2.1%. Inter-observer differences were: mitral annular area 4.9% ± 1.1 cm^2; tenting height 7.7% ± 0.9 mm; tenting volume 9.7% ± 0.4 mL; leaflet surface area 5.6% ± 1.5 cm^2; and co-aptation index 9.8 ± 4.6%.

Discussion

This study has characterized the functional–anatomical changes that occur in patients with left atrial dilatation and associated MR. Using 3D TOE, we have defined the underlying mechanism of valvular

Downloaded from https://academic.oup.com/ehjcimaging/article/15/5/500/2399644 by U.S. Department of Justice user on 17 August 2022

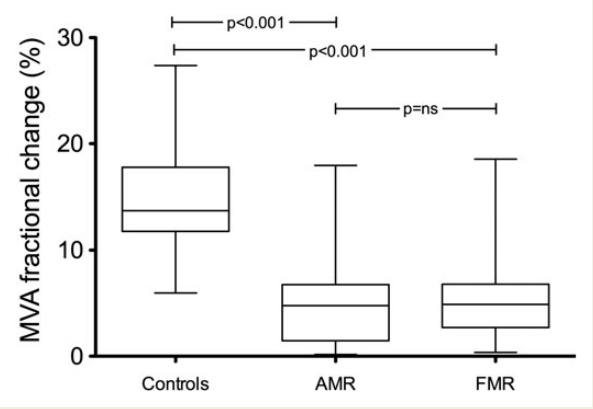

Figure 5 Box and whisper plot of MVA fractional change for the three study groups. Vertical bars represent range; box represents inter-quartile range, and horizontal line represents the mean. Abbreviations as previously.

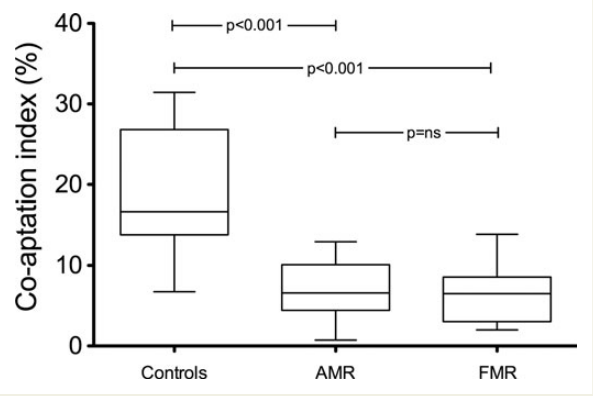

Figure 6 Box and whisper plot of the co-aptation values for the three study groups. Vertical bars represent range; box represents inter-quartile range, and horizontal line represents the mean. Abbreviations as previously.

insufficiency as a loss of leaflet co-aptation, which, in part, relates to reduced mitral annular fractional change. The co-aptation index is significantly related to the presence of MR in patients with functional or atrial MR, and left atrial volume is independently associated with annular size and function.

FMR is well described, occurring in patients with global or regional LV dysfunction.[4–7] Dilatation of the mitral annulus contributes to MR, but the most important anatomical alteration promoting valvular insufficiency is abnormal leaflet geometry and tethering. As the LV dilates, the mitral subvalve is displaced into the ventricle, preventing optimal valvular function: indeed, some authors have demonstrated that LV dysfunction in the absence of LV dilatation fails to produce important MR in experimental models.[8] Several echocardiographic measures describe the displacement of the subvalvular apparatus, in particular the tenting area.[18,19] The final common functional consequence of these anatomical changes is reduced leaflet co-aptation, and 3D echocardiography facilitates comprehensive assessment of the mitral valve with direct measurement of leaflet apposition. The co-aptation index has previously been used to describe the loss of co-aptation of the mitral leaflets in animal models of FMR,[9] where a value of $<12\%$ predicted the presence of important MR. In our study, $\leq 13\%$ was the cut-off displaying optimal sensitivity and specificity. More importantly, the application of this index to patients with MR and isolated left atrial dilatation confirms the mechanism of regurgitation in these individuals' to be loss of co-aptation, presumably as a consequence of mitral annular enlargement and impaired annular fractional change.

There is widespread appreciation that LV dilatation results in mitral annular enlargement.[4,7,20] The impact of the atrium on annular dimensions is less well established.[10–13] We suspect this is for several reasons. Previous work has noted that, for equivalent mitral annular size, patients with FMR had more valvular insufficiency than those with isolated LA dilatation.[10] The authors' conclusion was that isolated annular dilatation did not cause significant MR. Similarly, Zhou *et al.* studied patients with lone AF and concluded that although there was pronounced dilatation of the tricuspid valve annulus with associated TR, the effect on the mitral annulus was more modest, and significant MR did not occur.[13] In isolated atrial enlargement, if the annular dilatation is mild or moderate, the mitral leaflets can 'unfold' to maintain co-aptation and compensate for the increased annular size. This is reflected in the reduced tenting height seen in the AMR patients (*Figure 7*). This is not surprising: it has long been known that there is substantial leaflet surplus relative to the mitral orifice size.[21,22] Above a certain threshold, however, the leaflets can no longer overcome the increased annular dimensions, and mitral insufficiency will ensue. An important conclusion from our data is that the atrium appears to be the key association of mitral annular size. Linear regression analysis confirmed that LA volume was the strongest independent associate of MVA, whereas no such association was seen with LV dimensions. This suggests that annular dilatation seen in patients with FMR may be related to the presence of concurrent atrial enlargement in these patients. This requires further work and clarification. Of interest, and consistent with Zhou's observations, the majority of patients with AMR had evidence of moderate or worse TR, suggesting that co-existant right atrial enlargement and tricuspid annular dilatation occur in line with the observed changes in the mitral annulus.

In patients with AMR, the regurgitant jet was not focussed in one region, but was seen to be distributed along the length of the co-aptation zone, reflecting a generalized loss of apposition (*Figure 8*). This is analogous to the pattern seen in FMR, where it has been noted that the PISA is elongated and not spherical as is observed with mitral valve prolapse.[23] It is accepted that, in FMR, the threshold value of EROA indicating the presence of severe MR should be 0.20 cm^2 to account for this. Given the similar pattern of valvular insufficiency in AMR, we believe that a similar threshold would be suitable for these patients, but requires further study.

Describing the mitral valve annulus at a single time-point neglects the fact it is a dynamic structure that undergoes complex conformational alterations during the cardiac cycle. A substantial body of work confirms that the mitral annulus enlarges during systole and

Downloaded from https://academic.oup.com/ehjcimaging/article/15/5/500/2399644 by U.S. Department of Justice user on 17 August 2022

Table 3 Univariate and multivariate associations of mitral annular area and fractional change

Variables	Univariate		Multivariate	
	r	*P*-value	*β* (95% CI)	*P*-value
Mitral annular area: $r^2 = 0.789$				
Age	0.245	0.022	−0.01 (−0.04–0.02)	0.497
Gender	**0.414**	**<0.001**	**1.53 (0.70–2.35)**	**<0.001**
Rhythm	**−0.512**	**<0.001**	**−1.24 (−2.24–−0.24)**	**0.016**
LVIDd	0.479	<0.001	0.70 (−0.34–1.74)	0.185
LVIDs	0.310	0.005	0.09 (−0.98–1.16)	0.862
EF	−0.132	0.141	0.01 (−0.04–0.06)	0.653
LAV	**0.841**	**<0.001**	**0.03 (0.02–0.04)**	**<0.001**
Annular contraction: $r^2 = 0.469$				
Age	−0.405	<0.001	−0.05 (−0.15–0.06)	0.380
Gender	−0.047	0.350	−0.16 (−2.73–2.41)	0.901
Rhythm	**0.606**	**<0.001**	**4.85 (1.73–7.97)**	**0.003**
LVIDd	−0.263	0.015	−0.60 (−3.85–2.64)	0.711
LVIDs	−0.232	0.028	0.56 (−2.77–3.89)	0.737
EF	0.249	0.020	0.08 (−0.07–0.23)	0.289
LAV	**−0.556**	**<0.001**	**−0.03 (−0.06–−0.002)**	**0.037**

Independent associations are displayed in bold.
LVIDd: left ventricular internal diameter in diastole; LVIDs: left ventricular internal diameter in systole; EF: ejection fraction; LAV: left atrial volume.

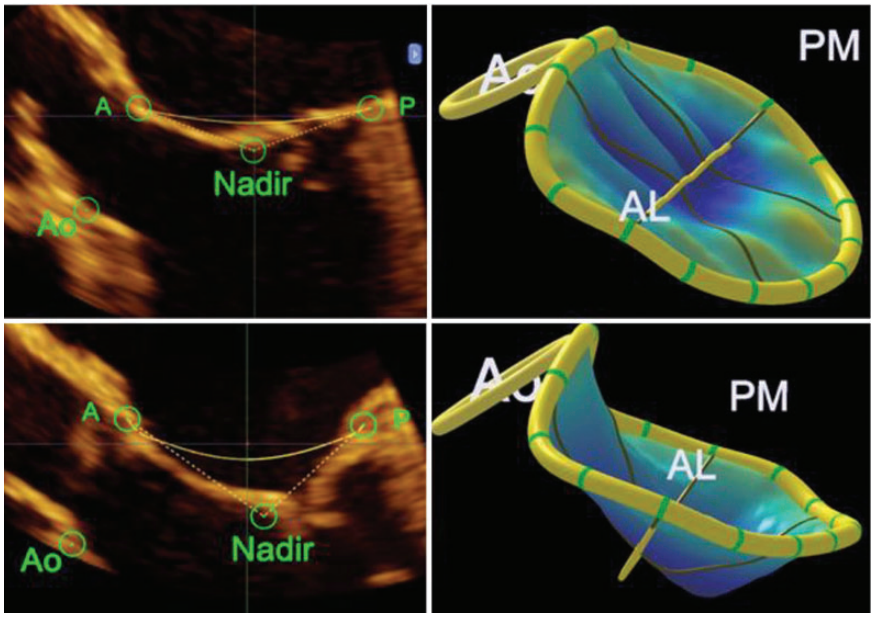

Figure 7 Mitral annular geometry in FMR and AMR. Top left pane depicts a 2D image of a patient with atrial MR. Note how the leaflets have 'unfolded' and sit close to the annular plane. This can also be seen in the cartoon image of the mitral annulus produced using MVQ analysis (top right). Conversely, in functional MR, the leaflets are tethered by the displaced subvalve and accordingly sit well below the level of the annulus. This can be seen in both the 2D image and mitral annular cartoon (bottom left and right, respectively). AL: anterolateral; PM: posteromedial; Ao: aorta.

contracts in diastole: the area of the annulus is smallest at the point of mitral valve closure, which may help in promoting optimal apposition of the leaflets.[24–28] Experimental work in sheep has linked atrial function to pre-systolic annular contraction: rapid atrial pacing in experimental animals increased volume change in the LA, which corresponded to a similar increase in mitral annular fractional change.[28] In a

Downloaded from https://academic.oup.com/ehjcimaging/article/15/5/500/2399644 by U.S. Department of Justice user on 17 August 2022

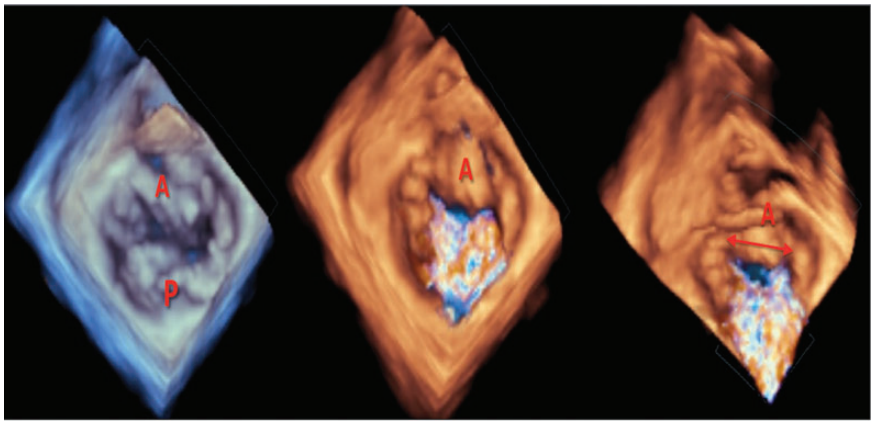

Figure 8 Pattern of regurgitation in patients with atrial MR. On the left is a full-volume acquisition of a mitral valve taken in mid-systole, with colour Doppler removed. Centre pane shows the valve at the same time-point with colour Doppler restored. Note how the regurgitant jet originates along the line of co-aptation. On the right, the image has been tilted. Again note how the regurgitant jet is visible along almost the entire length of co-aptation (arrow). A: anterior leaflet; P: posterior leaflet.

separate study, LV pacing eliminated both atrial contraction and pre-systolic mitral annular reduction.[26] Our current study in humans supports these previous observations. In AMR patients, fractional annular change was reduced similar to the value seen in FMR. After multivariate analysis, we demonstrated that the presence of AF and LA volume were key associations with reduced MVA fractional change, whereas no association was seen with LV size or function.

It seems likely that atrial enlargement is a more important cause of MR than has previously been considered.[10–12] We wonder whether AMR is synonymous with the syndrome of pure annular dilatation,[29] which has been noted to be a substantial cause of MR requiring surgical intervention.[30] This raises questions in our approach to patients with LA dilatation, and in particular those with AF. Management of AF is often limited to optimizing ventricular rate and anticoagulation strategies, but possibly attempts to restore sinus rhythm should be made in more patients. Recent work clearly demonstrated that this approach could lead to reduction in LA size and with it an improvement in the severity of MR.[14] We believe that it is, therefore, important to recognize AMR as a distinct entity with characteristic mitral annular geometry that requires a unique approach to its management. Surgical approaches to FMR frequently involve techniques designed to restore normal subvalve geometry and ventricular shape in addition to restrictive annuloplasty.[31–33] In AMR, these strategies would likely be unnecessary, and restrictive annuloplasty alone may be sufficient, along with surgical strategies to restore sinus rhythm.

Limitations

This is a single-centre study with limited numbers of patients and should be considered hypothesis-generating. Fasting patients, prior to TOE, may impact on volaemic status and measurements made of the mitral annulus. Frame rates and inter-observer variability may impact on the reproducibility of these results. Quantification of MR severity in AF and AMR is problematic due to the variable stroke volume, as regurgitation originates along the line of apposition and is not focussed in one region. Threshold for defining severe MR in these patients need further clarification.

Conclusion

Left atrial enlargement leads to mitral annular dilatation and reduced mitral annular fractional change, even in the absence of LV enlargement. This can result in important MR. Using 3D TOE-derived co-aptation index, we have demonstrated that the mechanism of MR in these patients is loss of optimal apposition of the mitral leaflets. Appreciating the importance of the atrium in the integrity of the mitral valve may lead us to re-address our approach to atrial dilatation and in particular AF, which is the main aetiological factor in this condition.

Conflict of interest: F.C.W. has a consultancy with St Jude Medical. D.P.D. receives research support from the Medical Research Council, the British Heart Foundation, and MSD. L.R., S.P.F., L.M.S., and B.S.R. have no conflicts of interest.

References

1. Trichon BH, Felker GM, Shaw LK, Cabell CH, O'Connor CM. Relation of frequency and severity of mitral regurgitation to survival among patients with left ventricular systolic dysfunction and heart failure. *Am J Cardiol* 2003;**91**:538–43.
2. Robbins JD, Maniar PB, Cotts W, Parker MA, Bonow RO, Gheorghiade M. Prevalence and severity of mitral regurgitation in chronic systolic heart failure. *Am J Cardiol* 2003;**91**:360–2.
3. Grigioni F, Enriquez-Sarano M, Zehr KJ, Bailey KR, Tajik AJ. Ischemic mitral regurgitation: long-term outcome and prognostic implications with quantitative Doppler assessment. *Circulation* 2001;**103**:1759–64.
4. He S, Fontaine AA, Schwammenthal E, Yoganathan AP, Levine RA. Integrated mechanism for functional mitral regurgitation: leaflet restriction versus coapting force: in vitro studies. *Circulation* 1997;**96**:1826–34.
5. Godley RW, Wann LS, Rogers EW, Feigenbaum H, Weyman AE. Incomplete mitral leaflet closure in patients with papillary muscle dysfunction. *Circulation* 1981;**63**:565–71.

Downloaded from https://academic.oup.com/ehjcimaging/article/15/5/500/2399644 by U.S. Department of Justice user on 17 August 2022

6. Kono T, Sabbah HN, Rosman H, Alam M, Jafri S, Goldstein S. Left ventricular shape is the primary determinant of functional mitral regurgitation in heart failure. *J Am Coll Cardiol* 1992;**20**:1594–8.
7. Yiu SF, Enriquez-Sarano M, Tribouilloy C, Seward JB, Tajik AJ. Determinants of the degree of functional mitral regurgitation in patients with systolic left ventricular dysfunction: a quantitative clinical study. *Circulation* 2000;**102**:1400–6.
8. Otsuji Y, Handschumacher MD, Schwammenthal E, Jiang L, Song JK, Guerrero JL *et al.* Insights from three-dimensional echocardiography into the mechanism of functional mitral regurgitation: direct in vivo demonstration of altered leaflet tethering geometry. *Circulation* 1997;**96**:1999–2008.
9. Yamada R, Watanabe N, Kume T, Tsukiji M, Kawamoto T, Neishi Y *et al.* Quantitative measurement of mitral valve coaptation in functional mitral regurgitation: in vivo experimental study by real-time three-dimensional echocardiography. *J Cardiol* 2009;**53**:94–101.
10. Otsuji Y, Kumanohoso T, Yoshifuku S, Matsukida K, Koriyama C, Kisanuki A *et al.* Isolated annular dilation does not usually cause important functional mitral regurgitation: comparison between patients with lone atrial fibrillation and those with idiopathic or ischemic cardiomyopathy. *J Am Coll Cardiol* 2002;**39**:1651–6.
11. Tanimoto M, Pai RG. Effect of isolated left atrial enlargement on mitral annular size and valve competence. *Am J Cardiol* 1996;**77**:769–74.
12. Kihara T, Gillinov AM, Takasaki K, Fukuda S, Song J-M, Shiota M *et al.* Mitral regurgitation associated with mitral annular dilation in patients with lone atrial fibrillation: an echocardiographic study. *Echocardiography* 2009;**26**:885–9.
13. Zhou X, Otsuji Y, Yoshifuku S, Yuasa T, Zhang H, Takasaki K *et al.* Impact of atrial fibrillation on tricuspid and mitral annular dilatation and valvular regurgitation. *Circ J* 2002;**66**:913–6.
14. Gertz ZM, Raina A, Saghy L, Zado ES, Callans DJ, Marchlinski FE *et al.* Evidence of atrial functional mitral regurgitation due to atrial fibrillation. *J Am Coll Cardiol* 2011;**58**:1474–81.
15. Lang RM, Bierig M, Devereux R, Flachskampf F, Foster E, Pellikka PA *et al.* Recommendations for chamber quantification. *Eur J Echocardiogr* 2006;**7**:79–108.
16. Lancellotti P, Moura L, Piérard LA, Agricola E, Popescu BA, Tribouilloy C *et al.* European Association of Echocardiography. European Association of Echocardiography recommendations for the assessment of valvular regurgitation. Part 2: mitral and tricuspid regurgitation (native valve disease). *Eur J Echocardiogr* 2010;**11**:307–32.
17. Lang RM, Badano LP, Tsang W, Adams DH, Agricola E, Buck T *et al.* EAE/ASE recommendations for image acquisition and display using three-dimensional echocardiography. *Eur Heart J Cardiovasc Imaging* 2012;**13**:1–46.
18. Kumanohoso T, Otsuji Y, Yoshifuku S, Matsukida K, Koriyama C, Kisanuki A *et al.* Mechanism of higher incidence of ischemic mitral regurgitation in patients with inferior myocardial infarction: quantitative analysis of left ventricular and mitral valve geometry in 103 patients with prior myocardial infarction. *J Thorac Cardiovasc Surg* 2003;**125**:135–43.
19. Watanabe N, Ogasawara Y, Yamaura Y, Kawamoto T, Toyota E, Akasaka T *et al.* Quantitation of mitral valve tenting in ischemic mitral regurgitation by transthoracic real-time three-dimensional echocardiography. *J Am Coll Cardiol* 2005;**45**:763–9.
20. Veronesi F, Corsi C, Sugeng L, Caiani EG, Weinert L, Mor-Avi V *et al.* Quantification of mitral apparatus dynamics in functional and ischemic mitral regurgitation using real-time 3-dimensional echocardiography. *J Am Soc Echocardiogr* 2008;**21**:347–54.
21. Duplessis LA, Marchand P. The anatomy of the mitral valve and its associated structures. *Thorax* 1964;**19**:221–7.
22. McCarthy KP, Ring L, Rana BS. Anatomy of the mitral valve: understanding the mitral valve complex in mitral regurgitation. *Eur J Echocardiogr* 2010;**11**:i3–9.
23. Matsumura Y, Fukuda S, Tran H, Greenberg NL, Agler DA, Wada N *et al.* Geometry of the proximal isovelocity surface area in mitral regurgitation by 3-dimensional color Doppler echocardiography: difference between functional mitral regurgitation and prolapse regurgitation. *Am Heart J* 2008;**155**:231–8.
24. Grewal J, Suri R, Mankad S, Tanaka A, Mahoney DW, Schaff HV *et al.* Mitral annular dynamics in myxomatous valve disease: new insights with real-time 3-dimensional echocardiography. *Circulation* 2010;**121**:1423–31.
25. Levack MM, Jassar AS, Shang EK, Vergnat M, Woo YJ, Acker MA *et al.* Three-dimensional echocardiographic analysis of mitral annular dynamics: implication for annuloplasty selection. *Circulation* 2012;**126**:S183–8.
26. Glasson JR, Komeda M, Daughters GT, Foppiano LE, Bolger AF, Tye TL *et al.* Most ovine mitral annular three-dimensional size reduction occurs before ventricular systole and is abolished with ventricular pacing. *Circulation* 1997;**96**:II-115–22;discussion II-123.
27. Timek TA, Lai DT, Tibayan F, Daughters GT, Liang D, Dagum P *et al.* Atrial contraction and mitral annular dynamics during acute left atrial and ventricular ischemia in sheep. *Am J Physiol Heart Circ Physiol* 2002;**283**:H1929–35.
28. Timek TA, Lai DT, Dagum P, Green GR, Glasson JR, Daughters GT *et al.* Mitral annular dynamics during rapid atrial pacing. *Surgery* 2000;**128**:361–7.
29. Carpentier A, Chauvaud S, Fabiani JN, Deloche A, Relland J, Lessana A *et al.* Reconstructive surgery of mitral valve incompetence: ten-year appraisal. *J Thorac Cardiovasc Surg* 1980;**79**:338–48.
30. Glower DD, Bashore TM, Harrison JK, Wang A, Gehrig T, Rankin JS. Pure annular dilation as a cause of mitral regurgitation: a clinically distinct entity of female heart disease. *J Heart Valve Dis* 2009;**18**:284–8.
31. Solis J, Levine RA, Johnson B, Guerrero JL, Handschumacher MD, Sullivan S *et al.* Polymer injection therapy to reverse remodel the papillary muscles: efficacy in reducing mitral regurgitation in a chronic ischemic model. *Circ Cardiovasc Interv* 2010;**3**:499–505.
32. Messas E, Guerrero JL, Handschumacher MD, Conrad C, Chow CM, Sullivan S *et al.* Chordal cutting: a new therapeutic approach for ischemic mitral regurgitation. *Circulation* 2001;**104**:1958–63.
33. Gillinov AM, Cosgrove DM, Shiota T, Qin J, Tsujino H, Stewart WJ *et al.* Cosgrove-Edwards annuloplasty system: midterm results. *Ann Thorac Surg* 2000;**69**:717–21.

Downloaded from https://academic.oup.com/ehjcimaging/article/15/5/500/2399644 by U.S. Department of Justice user on 17 August 2022